Biomimetic Lithography

DOI: 10.1002/anie.200805145

Biomineralization Nanolithography: Combination of Bottom-Up and Top-Down Fabrication To Grow Arrays of Monodisperse Gold Nanoparticles Along Peptide Lines**

*Nurxat Nuraje, Samia Mohammed, Linglu Yang, and Hiroshi Matsui**

The superior physical properties of nanomaterials have stimulated the construction of complex architectures for use as nanometer-scale devices. Two major approaches—top-down and bottom-up assemblies—have been applied in the fabrication of these architectures. Top-down fabrication has been used for a longer time in microfabrication and is still a major technique for the production of electronics and optics; this process requires the creation of nanoscale patterns at precise positions.[1,2] Further miniaturization with the top-down approach is limited by the spatial resolution of lithography; its use in nanofabrication is also not cost-effective. The bottom-up fabrication overcomes these demands by achieving nanofabrication in high spatial resolution with cost-effective and robust self-assembly,[3–9] however, the difficulty of precisely immobilizing nanoscale building blocks limits its practical application. Therefore, the combination of top-down and bottom-up fabrications could integrate advantages of both techniques to create nanoscale architectures with the precise and robust fabrication of nanoscale building blocks on substrates.[10–24]

Herein, we combine top-down and bottom-up fabrications to grow arrays of monodisperse Au nanoparticles (AuNPs) on peptide lines patterned on substrates. Top-down fabrication was used for the patterning of peptides that can effectively mineralize AuNPs, bottom-up fabrication was then applied to grow AuNPs on the underlying peptide lines to produce an array of AuNP lines with high monodispersity. Although arrays of NP lines have previously been grown on peptides patterned by microfluidics or holograms,[10,11] our method could dramatically reduce the particle size on the peptide array to 5 nm in diameter. Another advantage of our integrated technique is its simplicity in dictating the number of AuNP lines on substrates; the number of AuNP lines was simply determined by the width of the mineralizing peptide lines that were patterned by nanolithography. We observed that the number of lines of close-packed AuNPs increased proportionally as the patterned lines of the mineralizing peptides became wider. This is one of the simplest methods to fabricate large-scale arrays of monodisperse nanoparticles that have a line width of less than 10 nm.

To develop arrays of AuNP-aligned wires, the gold-mineralizing HRE peptide (AHHAHHAAD)[25,26] was first patterned in a series of lines on an Au substrate by nanolithography (Figure 1 a–c). Au nanoparticles were then grown on this peptide array pattern by biomineralization (Figure 1 d). After the Au substrate was incubated overnight with (2-(2-(2-(11-mercaptoundecyloxy)ethoxy)ethanol (MUEE, $SHC_{11}H_{22}(OCH_2CH_2)_3OH$) to form the protective self-assembled monolayer (SAM) that resists the nonspecific binding of peptides, a silicon atomic force microscope (AFM) cantilever was used as a pen to draw trenches by removing the MUEE SAMs from the Au substrate (Figure 1 b). After the formation of trenches was confirmed by AFM imaging (Figure 2 a), we immobilized 16-mercaptohexadeconic acid (MHA, a coupling agent that binds HRE peptides) in the trenches on the Au surface over a 12 hour incubation period, and then the HRE peptide was covalently bound to MHA in the trenches by using the 1-ethyl-3-(3-dimethylaminopropyl)-1-carbodiimide hydrochloride/N-hydroxysuccinimide (EDC/NHS) coupling reaction (Figure 1 c). After incubating the resulting substrate in $HAuCl_4$ for 24 hours, the Au ions on the HRE peptide were reduced with $NaBH_4$ for 2 hours in order to grow AuNPs on the HRE peptide lines (Figure 1 d).

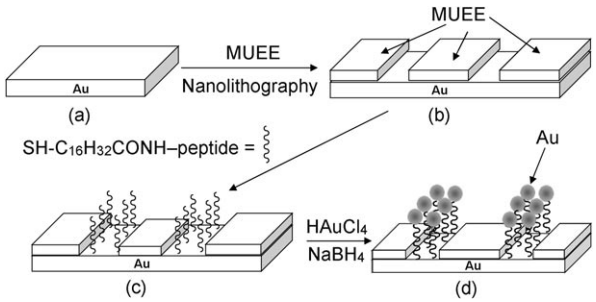

Figure 1. Growth of Au nanoparticle wires on Au substrates by mineralizing Au nanoparticles on the underlying HRE peptide array.

To study the correlation between the morphology of the AuNP arrays and the width of the mineralizing peptide lines, three different trench sizes (12 nm, 18 nm, and 32 nm) were prepared. The accurate measurement of the particle size and trench width are critical for this study, however these values cannot be reliably determined from AFM images because the

[*] Dr. N. Nuraje, S. Mohammed, Dr. L. Yang, Prof. H. Matsui
Department of Chemistry and Biochemistry
City University of New York—Hunter College
695 Park Avenue, New York, NY 10065 (USA)
Fax: (+1) 212-650-3918
E-mail: hmatsui@hunter.cuny.edu

[**] This work was supported by the U.S. Department of Energy (DE-FG-02-01ER45935). Hunter College infrastructure is supported by the National Institutes of Health, the RCMI program (G12-RR-03037). N.N. thanks Drs. C. M. Drain and R. de la Rica for useful discussions.

Supporting information for this article is available on the WWW under http://dx.doi.org/10.1002/anie.200805145.

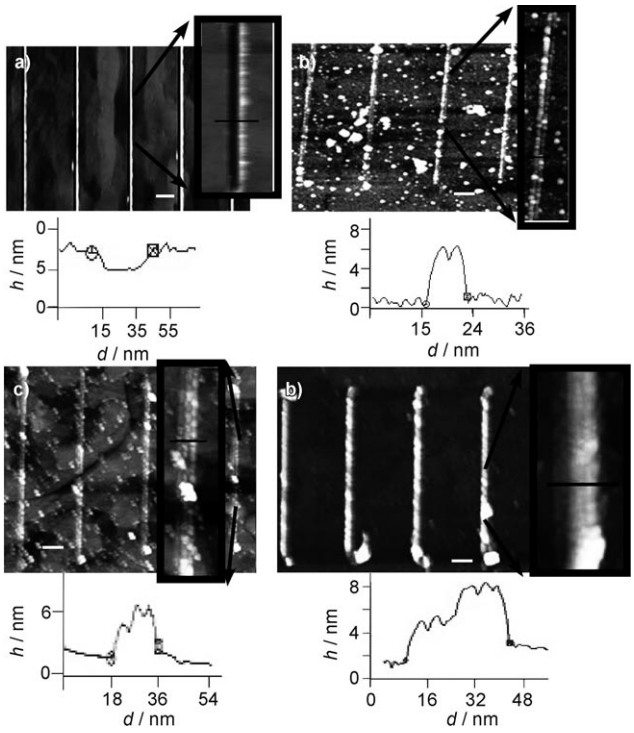

Figure 2. a) Top: AFM image of trenches patterned by AFM-based nanolithography. Bottom: Section analysis of the trench along the solid line. b) Top: AFM image of Au nanoparticles grown in the trenches of 12 nm width filled with HRE peptides. Bottom: Section analysis of the trench along the solid line. c) Top: AFM image of Au nanoparticles grown in the trenches of 18 nm width filled with HRE peptides. Bottom: Section analysis of the trench along the solid line. d) Top: AFM image of Au nanoparticles grown in trenches of 32 nm width filled with HRE peptides. Bottom: Section analysis of the trench along the solid line. Scale bar: 80 nm.

radius of the AFM tip is comparable to the size of the AuNPs. Since the particle radius was less than 4 nm from the height profile and the radius of the AFM tip was 15 nm, we applied the Zenhausern model to calibrate the scales in the *x*- and *y*-directions in all AFM images.[27] The Zenhausern model, which is one of the simplest quantitative evaluation methods to determine the dimensions of nanoscale features on surfaces, is especially suitable when the shape profile of the nanoscale objects is round and the radius of the nanoparticle is smaller than the radius of AFM tip.[28]

The diameter of the AuNPs in the trenches was found to be 5 nm when the same concentrations of $HAuCl_4$ and $NaBH_4$ were applied to trenches of different widths (Figure 2). However, the number of AuNP lines in each trench varied and increased as the HRE peptide lines widened. For example, when the peptide lines of 12 nm width were incubated with the Au precursor and the reducing agent, two lines of AuNPs of 5 nm diameter were grown on the peptide lines (Figure 2b). The section analysis of this trench in Figure 2b also shows two peaks, which correspond to the two AuNPs on the peptide lines. These AuNPs were close-packed and ordered, and the number of AuNP lines was proportional to the trench size. Three lines of AuNP wires were observed when the width of the peptide lines was increased to 18 nm, the corresponding section analysis also shows three peaks for those particles (Figure 2c). The number of AuNPs apparently increased further when the width of the peptide line was expanded to 32 nm as the corresponding section analysis indicates that five AuNP lines were formed in the 32 nm trenches (Figure 2d).

We hypothesized that the formation of AuNP arrays is controlled by the HRE peptide on the substrates. To confirm this hypothesis, we carried out a control experiment to reduce Au ions with the same reducing agent on the patterned Au substrate, but without conjugating the HRE peptide to the MHA SAMs in the trenches. Without the HRE peptides, no AuNPs were grown in the trenches (see the Supporting Information). In this control experiment, fewer AuNPs were observed in the background of the substrate (that is, non-trench regions), which indicates that the AuNPs in the background in Figure 1b–d arise from the contamination of the HRE peptide attached to the MUEE SAM. These results support the hypothesis that the HRE peptides are necessary to grow AuNPs in the trenches. As the AuNP size did not change and the number of lines increased as the peptide line width increased, we investigated the influence of the concentrations of both the peptide in the trenches and the Au precursors on the particle size and/or the number of AuNP lines. For example, MUEE or 16-mercaptohexadecane was introduced as a spacer in the trenches to reduce the concentration of HRE peptides on the surface. However, the growth of the AuNP lines was only observed in the trenches when the $HAuCl_4$ concentration was 0.1 mM and the spacers were not applied. The growth of metal nanoparticles on organic layers reflects complex factors such as the charge distribution on surfaces, the affinity of the peptide for metal ions, the precursor concentration, and the surface topology.[29,30] The growth conditions here seem to satisfy the ideal condition for the AuNP line formation, but unfortunately the exact mechanism for the growth of the close-packed AuNP lines from these complex conditions is still not well understood at this point. Since the HRE peptide contains many amino acids that bind strongly to Au ions, the fast nucleation of Au on the peptide lines could also contribute to the uniformity of the resulting Au NPs regardless of the line width. The topology of the trench is highly likely to be concave when the AFM tip scrapes the substrate for the nanolithography of the trench because of the tip shape, and the precise alignment of AuNPs along the trench direction could be assisted by the V-shaped cross section of the trench that results from the nanolithography process.

In conclusion, we have successfully demonstrated the fabrication of AuNP lines by mineralizing AuNPs on the HRE peptides that are patterned as line arrays by AFM nanolithography. The number of lines of AuNPs in the peptide-filled trench was simply determined by the width of the underlying gold-mineralizing HRE peptide patterns on the substrates. In the traditional fabrication of an monodisperse nanoparticle array, separately synthesized nanoparticles need to be assembled on substrates where binding motifs for capping ligands of nanoparticles are patterned.[31] Our biomineralization nanolithography approach reduces the number of fabrication steps for the nanoparticle-array formation by the direct growth of nanoparticles on substrates,

and the dimension of the lines could be reduced to less than 10 nm because of the mineralization function of peptides. The writing of AuNP lines by nanolithography could be applied to electronic components in the complicated designs of logic gates, and the fabrication of line arrays of the monodisperse nanoparticles could be useful in the fabrication of advanced photonic devices. The combination of biomineralization and nanolithography has a unique advantage in the creation of complex device geometries. The types of assembled nanoparticles can be expanded to semiconducting nanomaterials as various peptides were recently reported to behave as nanoreactors, which could catalyze semiconductor nanoparticle growths at room temperature.[32]

Experimental Section

Materials: EDC, NHS, 2-mercaptoethylamine, MHA, octadecanothiol, and $HAuCl_4$ were obtained from Aldrich, annealed gold substrates from Molecular Imaging, silicon substrates from Virginia Semiconductors, MUEE from SensoPath, HRE peptide (AAHAAHAAD) from Genescript, and Si_3N_4 AFM tips were purchased from MikroMasch.

Nanolithography: An array of the HRE peptide on Au substrates was patterned with AuNPs in the following sequence: Firstly, MUEE (1 mM, 2 mL) was self-assembled on Au substrates in 99% ethanol at room temperature for 12 h to prevent nonspecific binding of the HRE peptide (Figure 1a). When the substrate was taken out of the MUEE solution, it was diluted between five- and tenfold with ethanol and removed quickly to avoid multilayer formation. Then, an AFM cantilever was used as a pen to remove the SAM of MUEE to form trenches by the AFM nanolithography process (Figure 1b). Before writing the trenches, the substrate was washed three times with ethanol. After drying the resulting substrate in a stream of nitrogen, an array of trenches was written by removing the thiol SAMs by using the AFM tip. The nanolithography was carried out in air with a tip force of 1–3 μN in the contact mode with the scanning speed of 1 $\mu m s^{-1}$. In the next step, the substrate was immersed in 16-mercaptohexadecanoic acid (MHA)/ethanol solution (2 mL, 1 mM) overnight to assemble MHA molecules on the shaved trenches by thiol–gold interactions (Figure 1d). The substrate was taken out of the solution quickly after dilution with ethanol in the same manner as the MUEE SAM formation, in order to reduce multilayer deposition. After washing with ethanol and drying, the resulting substrate was incubated in an aqueous solution of NHS (50 mM, 1 mL) and EDAC (200 mM) for 15 min to form a covalent bond between the HRE peptide and the carbonyl group of MHA. The substrate was rinsed with ethanolamine (10 mM) and MES buffer (0.1 M) thoroughly, and then immersed in AAHAAHAAD HRE peptide (1 $mg mL^{-1}$, 1 mL) in a phosphate-buffered saline (PBS) solution (pH 7.4) for 12 h at 4 °C. After the substrate was passivated with a solution of ethanolamine (10 mM, 2 mL), it was rinsed with PBS buffer and then incubated in $HAuCl_4$ (0.1 mM, 3 mL) for one day. $NaBH_4$ (1%, 30 μL) was then added to reduce the Au ions and grow AuNPs on the HRE layer in the trenches. The substrate was removed from the growth solution after incubating for two hours and was rinsed with water upon removal. Finally, the substrate was dried in a stream of nitrogen gas. The topology of the resulting substrates was examined by AFM in tapping mode.

Received: October 21, 2008
Published online: February 18, 2009

Keywords: biomineralization · gold · nanolithography · nanostructures · peptides

[1] R. F. Pease, S. Y. Chou, *Proc. IEEE* **2008**, *96*, 248.
[2] Z. H. Nie, E. Kumacheva, *Nat. Mater.* **2008**, *7*, 277.
[3] W. Lu, C. M. Lieber, *Nat. Mater.* **2007**, *6*, 841.
[4] S. Liu, J. B.-H. Tok, J. Locklin, Z. Bao, *Small* **2006**, *2*, 1448.
[5] S. G. Rao, L. Huang, W. Setyawan, S. H. Hong, *Nature* **2003**, *425*, 36.
[6] P. A. Smith, C. D. Nordquist, T. N. Jackson, T. S. Mayer, B. R. Martin, J. Mbindyo, T. E. Mallouk, *Appl. Phys. Lett.* **2000**, *77*, 1399.
[7] U. Feldkamp, C. M. Niemeyer, *Angew. Chem.* **2006**, *118*, 1888; *Angew. Chem. Int. Ed.* **2006**, *45*, 1856.
[8] M. Boncheva, G. M. Whitesides, *MRS Bull.* **2005**, *30*, 736.
[9] C. S. Ozkan, Z. L. Wang, *Small* **2006**, *2*, 1322.
[10] R. R. Naik, S. J. Stringer, G. Agarwal, S. E. Jones, M. O. Stone, *Nat. Mater.* **2002**, *1*, 169.
[11] L. L. Brott, R. R. Naik, D. J. Pikas, S. M. Kirkpatrick, D. W. Tomlin, P. W. Whitlock, S. J. Clarson, M. O. Stone, *Nature* **2001**, *413*, 291.
[12] A. L. Briseno, J. Aizenberg, Y. J. Han, R. A. Penkala, H. Moon, A. J. Lovinger, C. Kloc, Z. A. Bao, *J. Am. Chem. Soc.* **2005**, *127*, 12164.
[13] S. Bhaviripudi, E. Mile, S. A. Steiner, A. T. Zare, M. S. Dresselhaus, A. M. Belcher, J. Kong, *J. Am. Chem. Soc.* **2007**, *129*, 1516.
[14] D. Kisailus, Q. Truong, Y. Amemiya, J. C. Weaver, D. E. Morse, *Proc. Natl. Acad. Sci. USA* **2006**, *103*, 5652.
[15] I. Yamashita, H. Kirimura, M. Okuda, K. Nishio, K. I. Sano, K. Shiba, T. Hayashi, M. Hara, *Small* **2006**, *2*, 1148.
[16] P. A. Suci, M. T. Klem, F. T. Arce, T. Douglas, M. Young, *Langmuir* **2006**, *22*, 8891.
[17] J. Lu, T. Kopley, D. Dutton, J. Liu, C. Qian, H. Son, M. Dresselhaus, J. Kong, *J. Phys. Chem. B* **2006**, *110*, 10585.
[18] J. B. Pang, S. S. Xiong, F. Jaeckel, Z. C. Sun, D. Dunphy, C. J. Brinker, *J. Am. Chem. Soc.* **2008**, *130*, 3284.
[19] Z. R. R. Tian, J. Liu, H. F. Xu, J. A. Voigt, B. Mckenzie, C. M. Matzke, *Nano Lett.* **2003**, *3*, 179.
[20] N. Nuraje, I. A. Banerjee, R. I. MacCuspie, L. Yu, H. Matsui, *J. Am. Chem. Soc.* **2004**, *126*, 8088.
[21] X. M. H. Huang, R. Caldwell, L. M. Huang, S. C. Jun, M. Y. Huang, M. Y. Sfeir, S. P. O'Brien, J. Hone, *Nano Lett.* **2005**, *5*, 1515.
[22] Y. Cui, M. T. Bjork, J. A. Liddle, C. Sonnichsen, B. Boussert, A. P. Alivisatos, *Nano Lett.* **2004**, *4*, 1093.
[23] S. W. Chung, D. S. Ginger, M. W. Morales, Z. F. Zhang, V. Chandrasekhar, M. A. Ratner, C. A. Mirkin, *Small* **2005**, *1*, 64.
[24] M. T. Zin, H. Ma, M. Sarikaya, A. K. Y. Jen, *Small* **2005**, *1*, 698.
[25] J. M. Slocik, J. T. Moore, D. W. Wright, *Nano Lett.* **2002**, *2*, 169.
[26] R. Djalali, Y.-F. Chen, H. Matsui, *J. Am. Chem. Soc.* **2003**, *125*, 5873.
[27] F. Zenhausern, M. Adrian, B. T. Heggeler-Bordied, L. M. Eng, P. Descouts, *Scanning* **1992**, *14*, 212.
[28] Y. Wang, X. Y. Chen, *Ultramicroscopy* **2007**, *107*, 293.
[29] J. Aizenberg, A. J. Black, G. M. Whitesides, *Nature* **1999**, *398*, 495.
[30] J. Aizenberg, D. A. Muller, J. L. Grazul, D. R. Hamann, *Science* **2003**, *299*, 1205.
[31] N. Nuraje, K. Su, J. Samson, A. Haboosheh, R. I. MacCuspie, H. Matsui, *Supramol. Chem.* **2006**, *18*, 429.
[32] X. Gao, H. Matsui, *Adv. Mater.* **2005**, *17*, 2037.

